Simultaneous Delivery of siRNA and Paclitaxel *via* a "Two-in-One" Micelleplex Promotes Synergistic Tumor Suppression

Tian-Meng Sun,[†,‡] Jin-Zhi Du,[†,§] Yan-Dan Yao,[†,⊥] Cheng-Qiong Mao,[‡] Shuang Dou,[‡] Song-Yin Huang,[⊥] Pei-Zhuo Zhang,[∥] Kam W. Leong,[#] Er-Wei Song,[⊥,*] and Jun Wang[‡,*]

[‡]Hefei National Laboratory for Physical Sciences at Microscale and School of Life Sciences, University of Science and Technology of China, Hefei, Anhui 230027, P.R. China, [§]CAS Key Laboratory of Soft Matter Chemistry and Department of Polymer Science and Engineering, University of Science and Technology of China, Hefei, Anhui 230026, P.R. China, [⊥]Sun-Yat-Sen Memorial Hospital, Sun-Yat-Sen University, Guangzhou, Guangdong 510120, P.R. China, [∥]Suzhou GenePharma Co., Ltd, Suzhou, Jiangsu 215123, P. R. China, and [#]Department of Biomedical Engineering, Duke University, Durham, North Carolina 27708, United States. [†]These authors contributed equally to this work.

ABSTRACT Combination of two or more therapeutic strategies with different mechanisms can cooperatively prohibit cancer development. Combination of chemotherapy and small interfering RNA (siRNA)-based therapy represents an example of this approach. Hypothesizing that the chemotherapeutic drug and the siRNA should be simultaneously delivered to the same tumoral cell to exert their synergistic effect, the development of delivery systems that can efficiently encapsulate two drugs and successfully deliver payloads to targeted sites *via* systemic administration has proven to be challenging. Here, we demonstrate an innovative "two-in-one" micelleplex approach based on micellar nanoparticles of a biodegradable triblock copolymer poly(ethylene glycol)-*b*-poly(ε-caprolactone)-*b*-poly(2-aminoethyl ethylene phosphate) to systemically deliver the siRNA and chemotherapeutic drug. We show clear evidence that the micelleplex is capable of delivering siRNA and paclitaxel simultaneously to the same tumoral cells both *in vitro* and *in vivo*. We further demonstrate that systemic administration of the micelleplex carrying polo-like kinase 1 (Plk1) specific siRNA and paclitaxel can induce a synergistic tumor suppression effect in the MDA-MB-435s xenograft murine model, requiring a thousand-fold less paclitaxel than needed for paclitaxel monotherapy delivered by the micelleplex and without activation of the innate immune response or generation of carrier-associated toxicity.

KEYWORDS: micelleplex · nanoparticle · siRNA delivery · codelivery · synergistic effect · cancer therapy

Cancer therapy relying on a single therapeutic strategy remains suboptimal. The combination of two or more therapeutic approaches with different mechanisms can cooperatively prohibit cancer development and is a promising strategy for effective treatments of cancers with synergistic or combined effects.[1−6] Meanwhile, considerable effort has been devoted to advanced therapeutics based on RNA interference, and a variety of siRNA-based therapeutics have been developed, showing great promise in disease treatments.[7−13] Therefore, the combination of traditional chemotherapy with newly emerging siRNA-based therapy has gained more attentions. For example, Spänkuch *et al.* have identified that treatment of breast cancer cells with siRNAs or antisense oligonucleotides targeting polo-like kinase 1 (Plk1) improved the sensitivity of cancer cells to paclitaxel.[14,15] Brahmbhatt *et al.* have reported that sequential administration of targeted minicells containing specific siRNA or a cytotoxic drug showed more significant therapeutic efficiency in the treatment of drug-resistant tumors than single administration of minicells loaded with siRNA or chemotheraputics.[16] Nevertheless, to exert their maximal effect *in vivo*, it is expected the chemotherapeutic drug and the siRNA should be simultaneously delivered to the same tumoral cell after systemic administration and, ideally, be distributed in the cells at an optimized ratio for maximal intracellular cooperation.

Advancement in nanotechnology has allowed for the development of delivery systems with dual capacity for siRNA and chemotherapeutic drugs. Minko and coworkers have reported the codelivery of siRNA and doxorubicin using liposome as a carrier for enhancing the efficacy of chemotherapy in the treatment of multidrug resistant cancer.[17] Mesoporous silica nanoparticles have also been fabricated as delivery systems for coencapsulation of siRNA targeting Bcl-2 or P-glycoprotein with doxorubicin to overcome drug resistance in cancer cell lines.[18,19] Moreover, nanoparticles derived from polymeric materials have been tested as carriers for simultaneous delivery of siRNA and anticancer drugs.[20−22] Nevertheless, although these carriers have

*Address correspondence to jwang699@ustc.edu.cn, songerwei02@yahoo.com.cn.

Received for review December 7, 2010 and accepted December 22, 2010.

Published online January 04, 2011
10.1021/nn103349h

shown potential *in vitro*, their performance *in vivo*, particularly following systemic administration, has not been reported.

Highly efficient and safe delivery systems which are suitable for systemic delivery of siRNA remain a major hurdle for RNA-based cancer therapy. Whereas, more sophisticated delivery systems are needed for combination therapies involving siRNA since they should have dual or multiple drug loading capacity as well as satisfying the systemic delivery. Until now, very limited work has been reported on the *in vivo* applications of codelivery of therapeutic siRNA and chemotherapeutic drugs for cancer therapy. The first study, reported by Huang's group, demonstrated that development of both cationic and anionic liposome-polycation−DNA (LPD) nanoparticles for systemic codelivery of siRNA and doxorubicin to the drug-resistant tumors; this system has achieved considerable therapeutic effects in a human lung cancer model.[23,24] Another example of this therapeutic paradigm is nanoparticles based on poly(D,L-lactide-co-glycolide) which have been used to codeliver paclitaxel along with siRNA targeting P-glycoprotein to drug resistant murine mammary cancer.[25] Nonetheless, the pursuit of potent and safe codelivery systems continues.

We have recently developed a micelleplex system based on the assembly of a biodegradable triblock copolymer poly(ethylene glycol)-*b*-poly(ε-caprolactone)-*b*-poly(2-aminoethyl ethylene phosphate) designated as mPEG-*b*-PCL-*b*-PPEEA. The triblock copolymer is amphiphilic and can self-assemble into micellar nanoparticles, with PCL as the hydrophobic core, PPEEA as the cationic shell and PEG as the hydrophilic corona.[26] The unique structure imparts these micellar nanoparticles with the capacity to simultaneous encapsulation of negatively charged siRNA and the hydrophobic paclitaxel to form a "two-in-one" micelleplex (Figure 1A). We examined the ability of this micelleplex to simultaneously deliver Plk1 specific siRNA (si*Plk1*) and paclitaxel into the same tumor cells both *in vitro* and *in vivo*, and further demonstrated the synergistic tumor suppression effect following systemic administration. We provide clear evidence that the "two-in-one" micelleplex system including a chemotherapeutic drug and specific siRNA cooperatively inhibits the tumor growth in a synergistic manner.

RESULTS AND DISCUSSION

In the present work, we synthesized the triblock copolymer designated as $mPEG_{45}$-*b*-PCL_{80}-*b*-$PPEEA_{10}$ (the subscript number represents degree of polymerization of each block) using a previously reported procedure.[26] The chemical structure of $mPEG_{45}$-*b*-PCL_{80}-*b*-$PPEEA_{10}$ is given in Figure 1A. The polymer formed a micellar structure in aqueous solution and exhibited the ability of simultaneous loading of siRNA and paclitaxel. Paclitaxel was entrapped in the hydrophobic PCL core with high encapsulation efficiency (>90%) *via* a hydrophobic−hydrophobic interaction (Figure 1B). si*Plk1* was subsequently absorbed to the assembly through a charge interaction with the PPEEA block to form the "two-in-one" micelleplex, denoted as $^{paclitaxel}micelleplex_{siPlk1}$. Efficient siRNA binding occurred at a molar ratio of nitrogen in the carrier/phosphate in siRNA (N/P ratio) of 5/1 as demonstrated by a gel retardation assay (Figure 1C). The micelleplex showed compact and spherical morphology with a mean diameter of 50 nm (Figure 1D, E), demonstrated by the transmission electronic microscopic image and dynamic light scattering analysis.

To demonstrate the simultaneous delivery, we first analyzed the cellular uptake and intracellular distribution of $^{Rho\text{-}paclitaxel}micelleplex_{FAM\text{-}siRNA}$ in MDA-MB-435s cells, where Rho-paclitaxel and FAM-siRNA represent rhodamine (Rho) and fluorescein (FAM) labeled paclitaxel and siRNA, respectively. Cells were incubated with $^{Rho\text{-}paclitaxel}micelleplex_{FAM\text{-}siRNA}$ for 1 or 2 h. Fluorescence-activated cell sorting (FACS) analysis showed that the cells were located only in the double-positive quadrant after 1 h incubation, indicating the micelleplex indeed delivered two payloads into the cells simultaneously. Furthermore, the intracellular fluorescence intensity increased with time as more micelleplexes were internalized (Figure 2A). Simultaneous delivery was corroborated by confocal microscopy, which showed a high degree of colocalization of the red and green fluorescence distributed in the cytoplasm (Figure 2B).

Herein, we verified whether the micelleplex could efficiently knockdown the expression of the therapeutic target gene Plk1. As previously reported, Plk1 is a key regulator of the mitotic progression in mammalian cells,[27,28] and the activity of Plk1 is elevated in cancer cells, which contributes to oncogenic transformation.[29] We incubated MDA-MB-435s cells with si*Plk1* packaged micelles ($micelleplex_{siPlk1}$) for 24 h and then detected Plk1 mRNA expression using real-time PCR. After sequence-specific Plk1 gene silencing by $micelleplex_{siPlk1}$, the Plk1 mRNA expression level was reduced in a si*Plk1* dose-dependent manner (Figure 3A). A higher si*Plk1* concentration resulted in more significant knockdown efficacy. For example, 62.5 and 125 nM of si*Plk1* led to approximately 32% and 78% knockdown of Plk1 mRNA, respectively, whereas negative controls including treatments with phosphate buffered saline (PBS, 0.01 M, pH7.4), blank micelle and micelle carrying scramble siRNA ($micelleplex_{siNonsense}$) showed no knockdown efficiency. Although transfection of MDA-MB-435s cells with Lipofectamine 2000 transfection reagent carrying 50 nM of si*Plk1* ($Lipofectamine_{siPlk1}$) exhibited more effective knockdown of Plk1 expression than with $micelleplex_{siPlk1}$ at 62.5 nM of si*Plk1*, it is worth noting that Lipofectamine 2000 is designated for *in vitro* transfection and not particularly suitable for

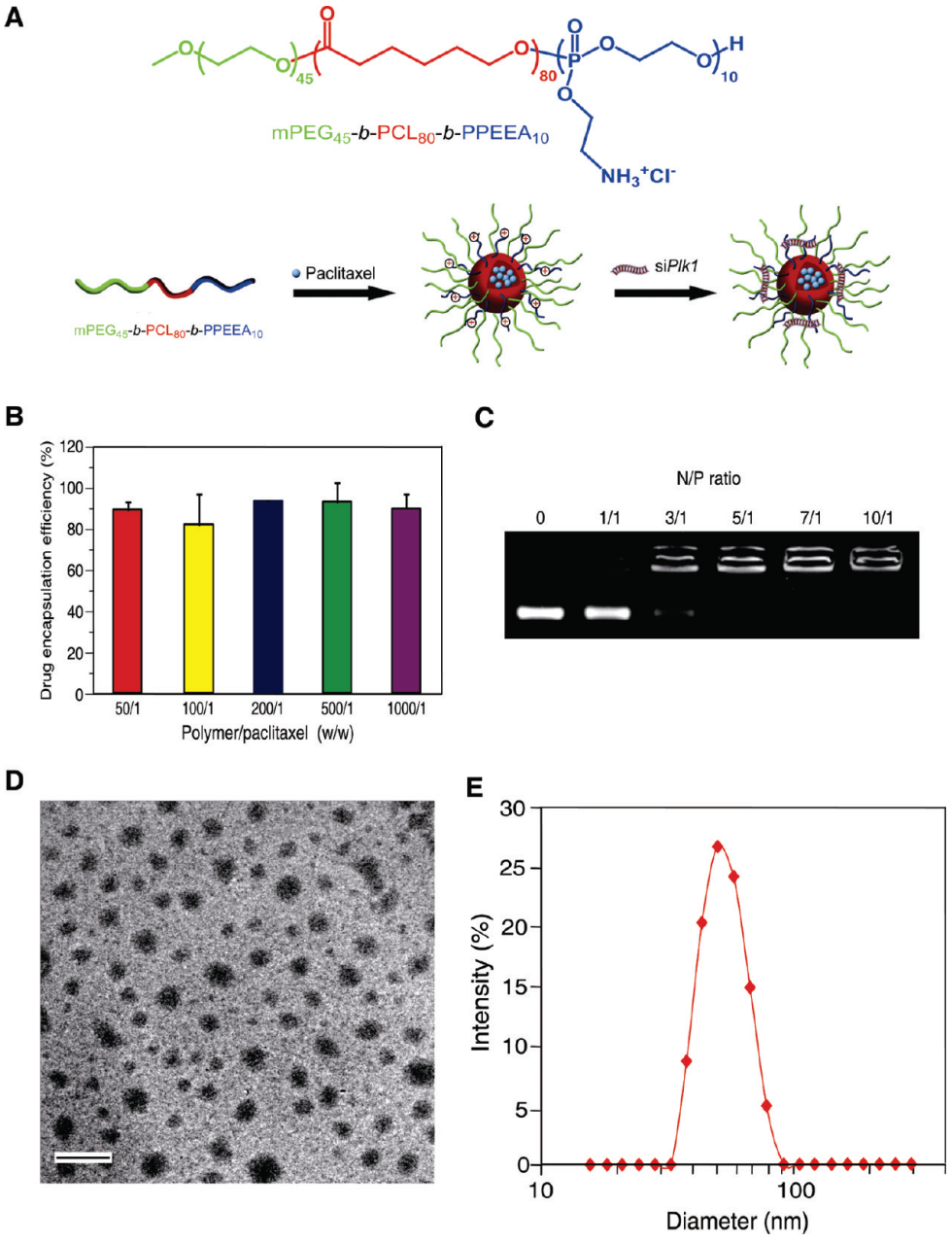

Figure 1. (A) Chemical structure of $mPEG_{45}$-*b*-PCL_{80}-*b*-$PPEEA_{10}$ and schematic illustration of micellar nanoparticle formation and the loading of paclitaxel and siRNA. (B) Paclitaxel encapsulation efficiency at various polymer to drug weight ratios ($n = 3$). (C) Binding ability of micellar nanoparticles to siRNA at different ratios of nitrogen in carrier to phosphate in siRNA (N/P ratio) demonstrated by the gel retardation assay. (D, E) Transmission electronic microscopic image (scale bar: 170 nm) and dynamic light scattering analysis of $^{paclitaxel}micelleplex_{siRNA}$ at a N/P ratio of 10/1.

in vivo applications. A reduction in Plk1 mRNA was subsequently accompanied by decreased Plk1 protein expression in a similar dose-dependent manner (Figure 3B, C) following transfection with $micelleplex_{siPlk1}$, as determined by Western blot analyses of Plk1 protein in the cell lysates 48 h after transfection.

Recently, Spänkuch and co-workers have reported that silencing Plk1 expression with si*Plk1* using commercial oligofectamine as a carrier improved the sensitivity of cells toward paclitaxel and Herceptin in a synergistic manner.[15] However, the synergistic effect on the inhibition of cell proliferation and induction of apoptosis was achieved by a two-step sequential treatment of cells with si*Plk1* and antineoplastic agents. Here, we sought to examine whether simultaneous delivery of si*Plk1* and paclitaxel by $^{paclitaxel}micelleplex_{siPlk1}$ could synergistically inhibit the proliferation of cancer cells. We incubated MDA-MB-435s cells with $^{paclitaxel}micelleplex_{siPlk1}$ at a fixed si*Plk1* dose (125 nM), while varying the dose of paclitaxel from 0.1 to 0.001 μg/mL. Cell proliferation was determined by a tritiated thymidine (^{3}H-TdR) incorporation assay. As indicated (Figure 4), simultaneous delivery of si*Plk1* with paclitaxel at a low concentration (0.005 μg/mL) by

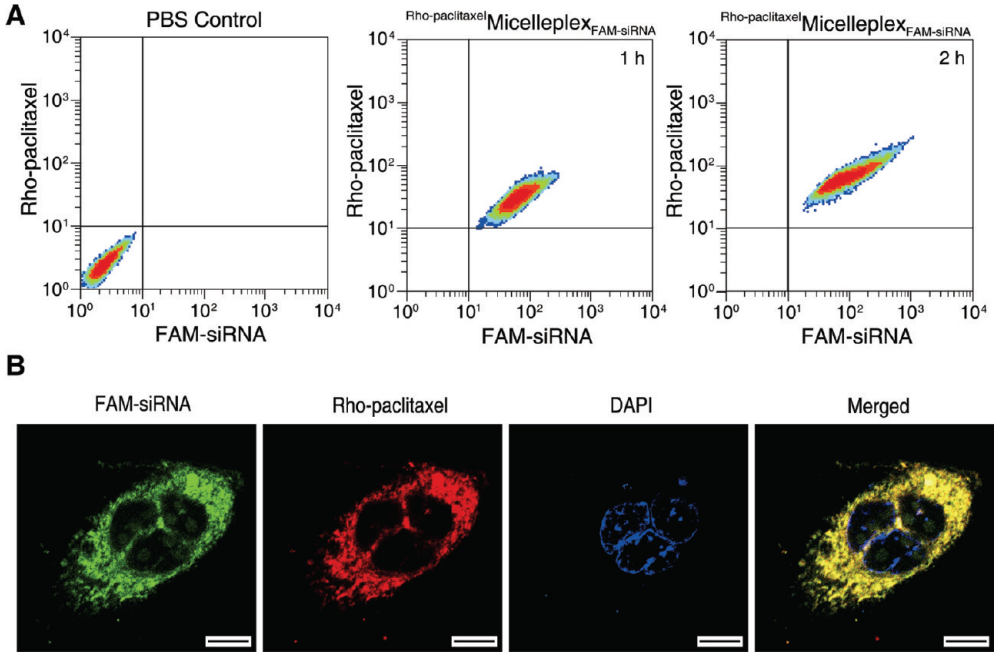

Figure 2. (A) Cellular uptake of $^{\text{Rho-paclitaxel}}$micelleplex$_{\text{FAM-siRNA}}$ over time as analyzed by fluorescence-activated cell sorting (FACS). (B) Confocal laser scanning microscope (CLSM) image of intracellular distribution of $^{\text{Rho-paclitaxel}}$micelleplex$_{\text{FAM-siRNA}}$ in MDA-MB-435s cell after incubation for 2 h (630×). The scale bar is 10 μm. Paclitaxel and siRNA were labeled with rhodamine (red) and fluorescein (green), respectively. Cell nuclei were stained with 4′,6-diamidino-2-phenylindole (DAPI; blue). Both FACS and CLSM analyses were performed after incubating $^{\text{Rho-paclitaxel}}$micelleplex$_{\text{FAM-siRNA}}$ with MDA-MB-435s at a N/P ratio of 10:1.

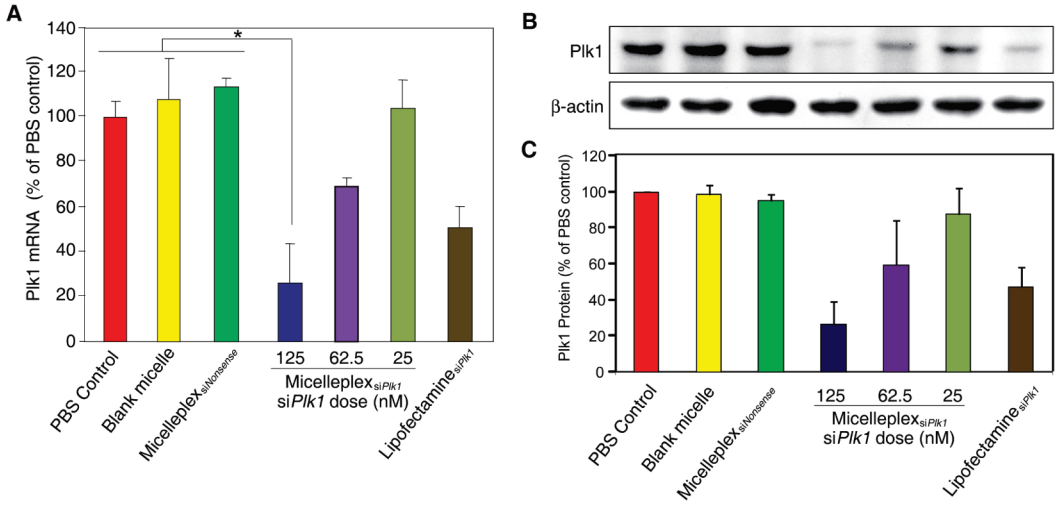

Figure 3. (A) Expression of Plk1 mRNA determined by quantitative real-time PCR. (B) Representative Plk1 protein expression determined by Western blot analysis. (C) Analysis of light intensities of Plk1 protein expression as the ratio of Plk1 to β-actin from Western blot results. MDA-MB-435s cells were transfected with micelleplex$_{\text{siPlk1}}$ at N/P of 10:1 with different si*Plk1* doses. The concentrations of si*Plk1* with Lipofectamine 2000 (Lipofectamine$_{\text{siPlk1}}$) and si*Nonsense* with micelleplex (micelleplex$_{\text{siNonsense}}$) were 50 and 125 nM, respectively. Transfection experiments were performed independently three times. * $p < 0.007$ as compared with controls ($n = 3$).

$^{\text{paclitaxel}}$micelleplex$_{\text{siPlk1}}$ significantly reduced cell proliferation to ~10%, achieving a synergistic inhibitory effect (combination index (*c.i.*) < 1), which was in sharp contrast to that induced by $^{\text{paclitaxel}}$micelleplex$_{\text{siNonsense}}$ (~50% inhibition, $p < 0.005$) and micelleplex$_{\text{siPlk1}}$ (~40% inhibition, $p < 0.003$). However, although combinatorial delivery of separate si*Plk1* and paclitaxel by $^{\text{paclitaxel}}$micelleplex$_{\text{siNonsense}}$ and micelleplex$_{\text{siPlk1}}$ also induced an obvious inhibition of cell proliferation, the extent was inferior to the simultaneous delivery system, especially with the concentration of paclitaxel at 0.01 and 0.005 μg/mL. In addition, it was observed that treatment with free paclitaxel dissolved in dimethyl sulfoxide (DMSO) at doses of 0.005 and 0.01 μg/mL showed less inhibitory effect on cell proliferation when compared with the micelleplex delivery system carrying

the same dose of paclitaxel, indicating that micelleplex can enhance the cytotoxicity of paclitaxel at certain doses. It is worth noting that blank micelles and micelleplex$_{siNonsense}$ did not exhibit a significant inhibitory effect on cell proliferation.

Knockdown of Plk1 has been shown to induce apoptosis in tumor cells.[30] Apoptosis was evaluated after treating MDA-MB-435s cells with formulations containing 0.005 μg/mL paclitaxel and/or 125 nM si*Plk1*, and then stained with Annexin-V-FITC and propidine iodide (PI) for the determination of cell apoptosis. Micelleplex$_{siPlk1}$ was able to induce cell apoptosis (including the early apoptotic cells and fully apoptotic cells) to ~16%, but not surprisingly, simultaneous delivery of si*Plk1* with paclitaxel at 0.005 μg/mL increased cell apoptosis to ~58%, with a synergistic effect as well (*c.i.* < 1, Figure 5), which was clearly higher than that of the combinatorial delivery system (^{paclitaxel}micelleplex$_{siNonsense}$+micelleplex$_{siPlk1}$, ~43%). Similarly to the cell proliferation assay described above, neither blank micelles nor micelleplex$_{siNonsense}$ induced significant cell apoptosis.

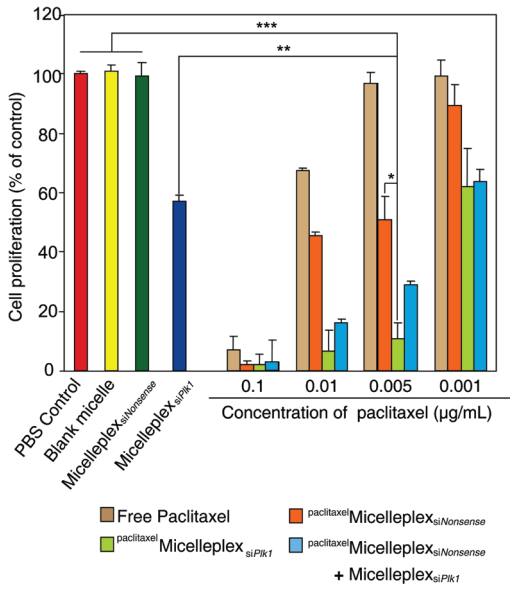

Figure 4. Effect of codelivery of si*Plk1* and paclitaxel by micelleplex on the proliferation of MDA-MB-435s cells. The concentration of paclitaxel varied from 0.001 to 0.1 μg/mL, while the concentration of both si*Plk1* and si*Nonsense* was 125 nM. Free paclitaxel was dissolved in DMSO for cell culture. * $p < 0.005$, ** $p < 0.003$, *** $p < 0.001$ ($n = 3$).

The nanosized micelleplex possesses a PEG protection corona, thus is expected to be beneficial for its accumulation in tumor site through the "enhanced permeation and retention" (EPR) effect, which is also called passive targeting of nanoparticulate delivery system.[31] To demonstrate this, we administrated $^{Rho\text{-}paclitaxel}$micelleplex$_{FAM\text{-}siRNA}$ by tail vein injection to MDA-MB-435s tumor-bearing mice and monitored the micelleplex distributions *in situ* by fluorescence imaging. The image revealed both rhodamine and fluorescein fluorescence at tumor site and within tumor tissue (Figure 6A and Supporting Information, Figure S1). More interestingly, when the fluorescence gradually faded from other parts of the body over time, it could still be detected at the tumor site. This demonstrated that the micelleplex could indeed enhance payload accumulation in tumor tissues. In contrast, fluorescence was completely absent within 4 h following the injection of free FAM-siRNA (Figure 6A).

To further examine whether $^{Rho\text{-}paclitaxel}$micelleplex$_{FAM\text{-}siRNA}$ can simultaneously deliver payloads into tumoral

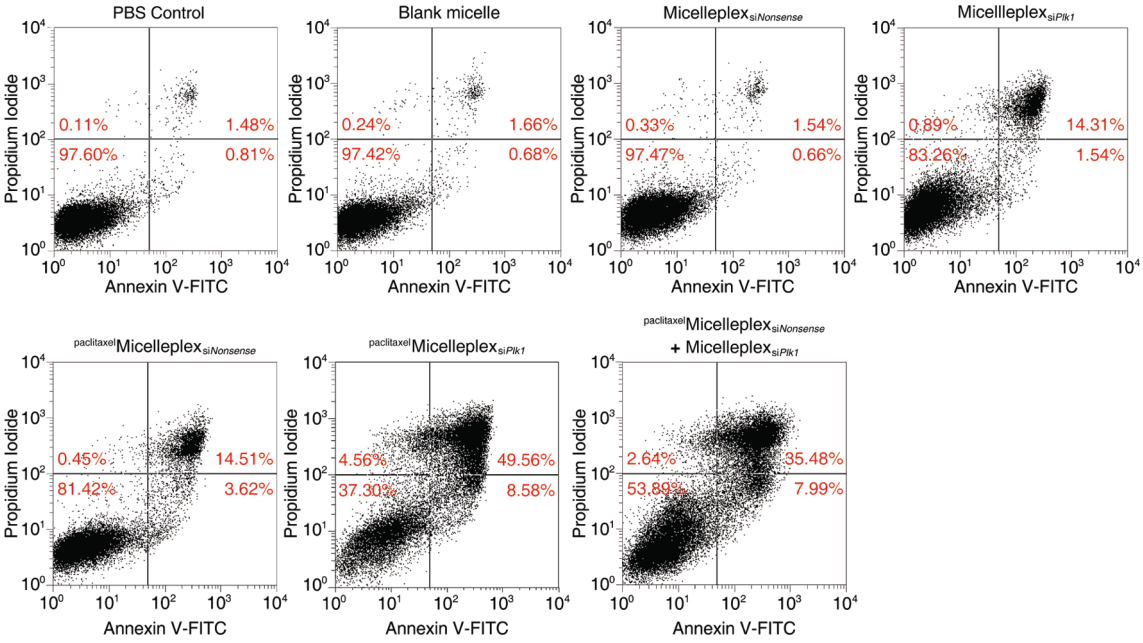

Figure 5. Induction of apoptosis on MDA-MB-435s cells by ^{paclitaxel}micelleplex$_{siPlk1}$ and other formulations. The early apoptotic cells are presented in the lower right quadrant, and fully apoptotic cells are presented in the upper right quadrant.

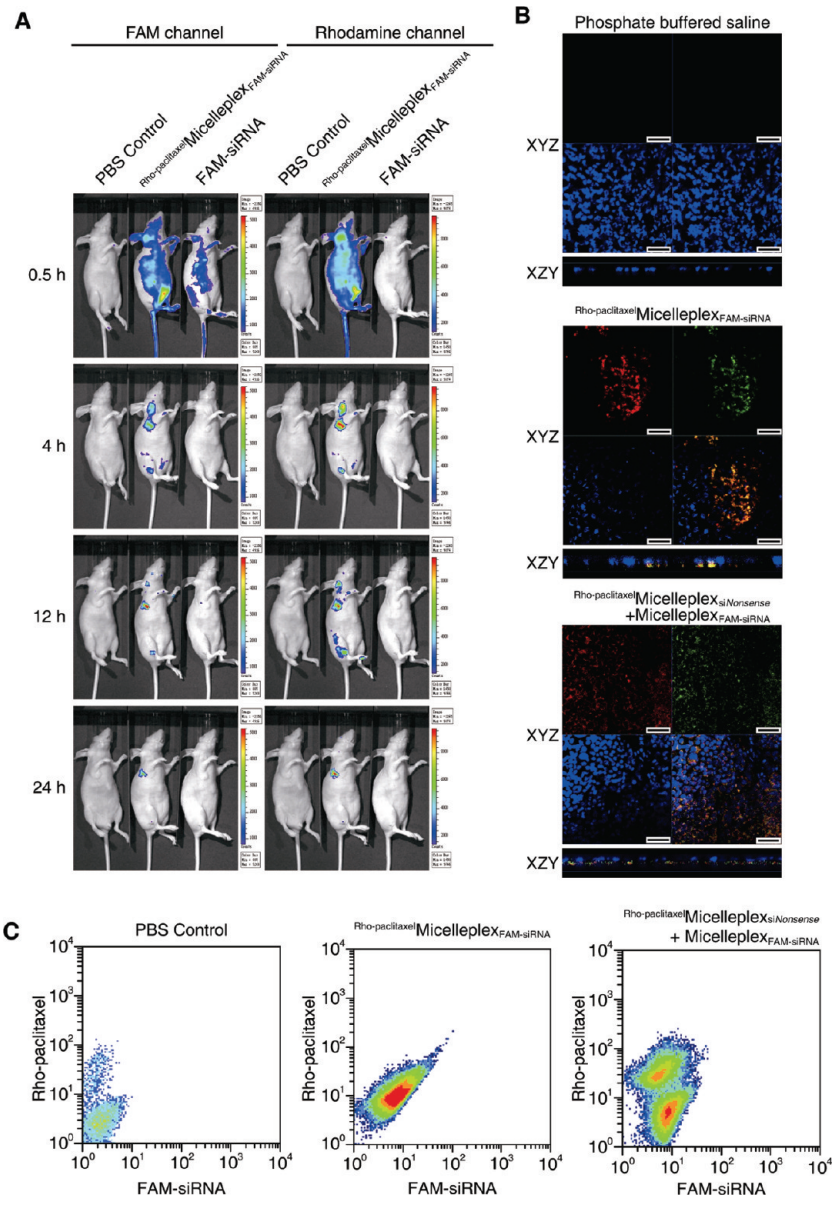

Figure 6. (A) Fluorescence images of MDA-MB-435s xenograft-bearing mice after intravenous (i.v.) injection of PBS, $^{\text{Rho-paclitaxel}}\text{micelleplex}_{\text{FAM-siRNA}}$ or free FAM-siRNA. (B) CLSM images show the distribution of paclitaxel and siRNA in tumor following i.v. injection of PBS, $^{\text{Rho-paclitaxel}}\text{micelleplex}_{\text{FAM-siRNA}}$ or $^{\text{Rho-paclitaxel}}\text{micelleplex}_{\textit{siNonsense}}$ and $\text{micelleplex}_{\text{FAM-siRNA}}$ (400×). Paclitaxel and siRNA were labeled with rhodamine (red) and fluorescein (green), respectively, and cell nuclei were stained with DAPI (blue). The scale bar is 50 μm. (C) FACS analysis of Rho-paclitaxel and FAM-siRNA colocalization in tumoral cells following i.v. injection of PBS, $^{\text{Rho-paclitaxel}}\text{micelleplex}_{\text{FAM-siRNA}}$ or $^{\text{Rho-paclitaxel}}\text{micelleplex}_{\textit{siNonsense}}$ and $\text{micelleplex}_{\text{FAM-siRNA}}$.

cells following its accumulation in tumor tissue, we sectioned the tumor tissues 24 h post injection. Confocal image exhibited strong and well colocalized Rho-paclitaxel and FAM-siRNA fluorescence in the tissue section (Figure 6B). The two fluorescent signals were primarily distributed around the nucleus according to the Z-scan analysis, indicating the simultaneous uptake of both payloads by tumoral cells with the delivery of the micelleplex. In contrast, although combinatorial administration of $^{\text{Rho-paclitaxel}}\text{micelleplex}_{\textit{siNonsense}}$ and $\text{micelleplex}_{\text{FAM-siRNA}}$ delivered Rho-paclitaxel and FAM-siRNA to tumor tissues, the fluorescent signals were less colocalized within tumoral cells (Figure 6B), implying that combinatorial delivery was less effective for the simultaneous delivery of paclitaxel and siRNA into the same tumoral cells *in vivo*.

This conclusion was also supported by FACS analysis of tumor cells following systemic administration (Figure 6C). We isolated tumor cells from the tumor tissue of mice 24 h postinjection and analyzed the cells by FACS. For $^{\text{Rho-paclitaxel}}\text{micelleplex}_{\text{FAM-siRNA}}$ injection, the distribution of tumoral cells was relatively concentrated and the majority of cells were located in the double-positive quadrant. However, with the combinatorial systemic delivery of $^{\text{Rho-paclitaxel}}\text{micelleplex}_{\textit{siNonsense}}$ and $\text{micelleplex}_{\text{FAM-siRNA}}$, tumoral cells were split into

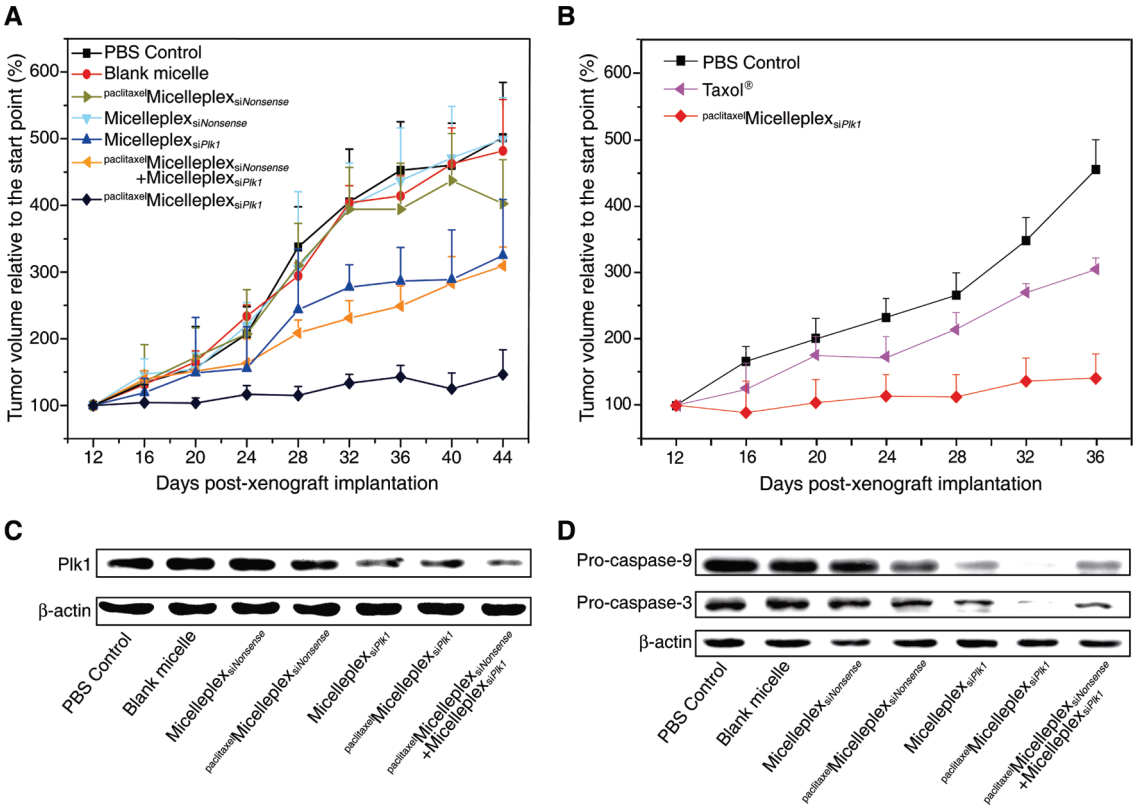

Figure 7. (A) Inhibition of MDA-MB-435s xenograft tumor growth by ^{paclitaxel}micelleplex$_{siPlk1}$ in comparison with various formulations (n = 6). (B) Comparison of tumor growth inhibition effect between i.v. injection of Taxol and ^{paclitaxel}micelleplex$_{siPlk1}$ with the same dose of paclitaxel (n = 6). (C) Western blot analyses of Plk1 protein in tumor after four injections of different formulations. (D) Western blot analyses of pro-caspase-9 and pro-caspase-3 after 17 injections of different formulations. MDA-MB-435s xenograft tumor-bearing mice received one i.v. injection every other day from the 12th day postxenograft implantation in all of the experiments. The dose of paclitaxel per injection was 0.667 μg/kg and the dose of siRNA was 0.223 mg/kg, if required. The tumor tissues were collected for Western blot analyses 24 h after the last injection.

two populations and the fraction of double-positive cells was significantly reduced. The results were in agreement with observation by CLSM, demonstrating that ^{paclitaxel}micelleplex$_{siPlk1}$ system was advantageous in simultaneous delivery of paclitaxel and siRNA into the same tumoral cells. Moreover, the presence of si*Plk1* in tumoral cells delivered by the micelleplex was clearly detected by *in situ* hybridization of si*Plk1*, which indicated that si*Plk1* was mainly distributed in the cytoplasm where the siRNA exerted its function (Supporting Information, Figure S2).

Next, we assessed whether the synergistic effect of ^{paclitaxel}micelleplex$_{siPlk1}$ on cell proliferation inhibition *in vitro* could also be achieved in terms of tumor growth inhibition following systemic administration. Mice bearing MDA-MB-435s xenografts were treated by ^{paclitaxel}micelleplex$_{siPlk1}$ or various other formulations through i.v. injection every other day from the 12th day after xenograft implantation. As indicated (Figure 7A), the delivery of paclitaxel by ^{paclitaxel}micelleplex$_{siNonsense}$ at a lower paclitaxel dose (0.667 μg/kg per injection) hardly affected tumor growth compared with PBS treatment. Delivery of si*Plk1* (0.223 mg/kg per injection) by micelleplex$_{siPlk1}$ only moderately inhibited tumor growth. However, simultaneous delivery of the same doses of paclitaxel and si*Plk1* by ^{paclitaxel}micelleplex$_{siPlk1}$ exhibited particularly significant inhibition of tumor growth compared with PBS treatment ($p < 0.0001$). More importantly, a synergistic inhibitory effect of the two therapeutic agents on tumor growth was demonstrated (*c.i.* < 1). In contrast, combinatorial delivery of separate si*Plk1* and paclitaxel by micelleplex$_{siPlk1}$ and ^{paclitaxel}micelleplex$_{siNonsense}$ only showed moderate inhibition of tumor growth and no synergistic effect was observed, primarily due to the more separate internalization of the two micelleplexes by tumoral cells as demonstrated above. Additionally, the codelivery system ^{paclitaxel}micelleplex$_{siPlk1}$ showed a more effective antitumor growth effect than Taxol with the same paclitaxel dose (Figure 7B). Taxol is a clinically used formulation of paclitaxel dissolved in Cremophor EL and 50% ethanol. It is worth noting that although the therapy was performed every other day, the overall dose of siRNA for injection in the whole therapeutic process was only 3.79 mg/kg (17 injections). Such a dose of siRNA was comparable to and even lower than the doses used in other reports.[24,32,33]

To determine if siRNA delivery by micelleplex affected the knockdown of the targeted mRNA *in vivo*, we treated mice bearing MDA-MB-435s xenografts

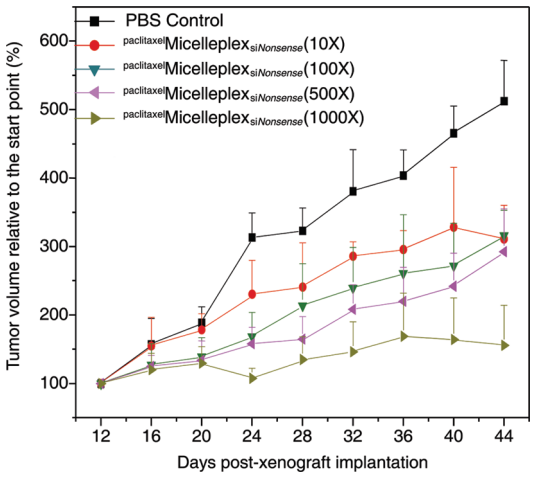

Figure 8. Dose−response study of paclitaxel delivered by ^{paclitaxel}micelleplex$_{siNonsense}$ on inhibition of MDA-MB-435s xenograft tumor growth (n = 6). Paclitaxel doses were 10 to 1000-fold increase (10× to 1000×) compared to those used in ^{paclitaxel}micelleplex$_{siPlk1}$. Tumor-bearing mice received one i.v. injection every other day from the 12th day post-xenograft implantation. The dose of si*Nonsense* per injection was 0.223 mg/kg, while the doses of paclitaxel per injection varied from 6.67 μg/kg (10×) to 667 μg/kg (1000×), respectively.

every other day with one injection of ^{paclitaxel}micelleplex$_{siPlk1}$ or the other controls. After four injections, the tumor mass was excised 24 h after the last injection and Plk1 mRNA expression was analyzed by quantitative real-time PCR. Xenografts from mice treated by the micelleplex containing si*Plk1* showed reduced Plk1 mRNA levels (~ 60% of the PBS control, Supporting Information, Figure S3), whereas the other controls did not cause this effect. Analysis of Plk1 protein of each tumor mass by Western blot showed consistent knockdown efficiency. Down-regulation of Plk1 protein occurred only when the micelleplex containing si*Plk1* was used (Figure 7C). It should also be noted that such a low dose of paclitaxel delivered by the micelleplex did not affect the Plk1 mRNA and protein expression.

The significant inhibition of ^{paclitaxel}micelleplex$_{siPlk1}$ on tumor growth was also supported by Western blot analyses of pro-caspase-3 and pro-caspase-9 in the tumor after treatment. Pro-caspase-3 and pro-caspase-9 were clearly activated by ^{paclitaxel}micelleplex$_{siPlk1}$ treatments in comparison to treatment with micelleplex$_{siPlk1}$ or combinatorial treatment with micelleplex$_{siPlk1}$ and ^{paclitaxel}micelleplex$_{siNonsense}$, indicating more significantly enhanced apoptosis following ^{paclitaxel}micelleplex$_{siPlk1}$ treatment (Figure 7D). In addition, the simultaneous delivery system remarkably increased TUNEL-positive tumoral cells (Supporting Information, Figure S4A) and reduced the percentage of proliferating Ki67-positive tumoral cells (Supporting Information, Figure S4B), indicating the enhanced efficiency of ^{paclitaxel}micelleplex$_{siPlk1}$ treatments in inducing apoptosis and inhibiting the proliferation of tumoral cells.

To further demonstrate the effectiveness of the simultaneous delivery system on tumor growth inhibition, we performed an *in vivo* tumor suppression experiment with the micelleplex by replacing si*Plk1* with si*Nonsense*, while increasing the paclitaxel dose from 10 to 1,000-fold over that used in ^{paclitaxel}micelleplex$_{siPlk1}$. Although a comparable therapeutic effect to ^{paclitaxel}micelleplex$_{siPlk1}$ could be achieved by single paclitaxel therapy with the delivery of micelleplex (^{paclitaxel}micelleplex$_{siNonsense}$), one thousand-fold or more paclitaxel was needed (Figure 8). This result demonstrates that the synergistic inhibitory effect of the simultaneous delivery system can significantly reduce the dose of antineoplastic drug required when delivered by the same micellar system.

It has been reported that double-stranded siRNA may activate the innate immune response, leading to a nonspecific antitumor effect.[34,35] To address this issue, mice bearing tumor xenografts were treated similarly to the antitumor efficacy experiments with four injections (one injection every other day), and then euthanized at 4 h (early response) and 24 h (late response) after the last injection. Serum was collected and assayed for human and mouse interferon (IFN) as well as inflammatory cytokines produced by the immune system. The results showed that, at both time points, delivery of si*Plk1* by the micelleplex did not cause an elevation in human or mouse IFN-α, IFN-β, IFN-γ, tumor necrosis factor (TNF)-α or interleukin (IL)-6 levels (Supporting Information, Figure S5). Additionally, simultaneous delivery of si*Plk1* and paclitaxel with the micelleplex did not result in any sign of toxicity to the mice as demonstrated by normal heart, liver and kidney functions following treatment (Supporting Information, Table S1). Collectively, the results established that the antitumor effect of ^{paclitaxel}micelleplex$_{siPlk1}$ was a result of the cooperation of the specific knockdown of Plk1 and the cytotoxicity of paclitaxel rather than due to siRNA-mediated activation of the innate immune response.

Although the combination of chemotherapy and siRNA-based therapy for cancer treatment has received increasing attention, the ideal delivery system that can maximize the efficiency of the active agents is a great challenge. It has been proposed that such delivery vehicles should: (i) be able to encapsulate different payloads with tunable doses, (ii) endow similar pharmacokinetics of the payloads and be able to systemically deliver them into the same tumoral cells, (iii) synergistically inhibit tumor growth following systemic injection, and (iv) be safe for *in vivo* applications. In this study, we developed an innovative "two-in-one" micelleplex for simultaneous delivery of Plk1-specific siRNA and paclitaxel for combination cancer therapy. We found that the two drugs delivered by the "two-in-one" micelleplex was able to fulfill the above criteria, and thus demonstrated that the micelleplex exerted a

synergistic tumor suppression effect *in vivo* following systemic administration. In contrast, combinatorial delivery of separate si*Plk1* and paclitaxel with the physical mixture of ^{paclitaxel}micelleplex$_{siNonsense}$ and micelleplex$_{siPlk1}$ could not deliver both drugs to the same tumoral cell at the optimized drug doses. As a result, the physical mixture could not induce a synergistic effect on tumor growth inhibition. In fact, as demonstrated *in vitro* (Figure 4), the drug ratio of si*Plk1* and paclitaxel was critical in achieving the synergistic antitumor effect. Further underlying mechanistic studies (Figure 6B, C) revealed that the "two-in-one" micelleplex could successfully deliver both siRNA and paclitaxel into the same tumoral cell at the designated drug ratio. However, with regard to the combinatorial delivery, siRNA and paclitaxel to a large extent were separately delivered to different tumoral cells, resulting in unpredicted intracellular drug distribution in individual tumoral cells.

CONCLUSION

In summary, this study represents the first example of systemic and simultaneous delivery of siRNA and a chemotherapeutic drug by micellar nanoparticles demonstrating synergistic tumor growth inhibition. The "two-in-one" micelleplex system shows great superiority in simultaneously delivering the two payloads into the same tumor cell, and can remarkably inhibit tumor growth in a synergistic manner. We have, for the first time, provided clear evidence that the synergistic tumor suppression effect is correlative to the simultaneous delivery of siRNA and paclitaxel into tumor cells. Additionally, the "two-in-one" micelleplex system is highly biocompatible and exhibits no activation of the innate immune response after systemic administration. We believe that the high effectiveness and biocompatibility of this simultaneous delivery system provides a promising approach for cancer therapy.

MATERIALS AND METHODS

Materials and Characterization. Paclitaxel and rhodamine-labeled paclitaxel (Rho-paclitaxel) were purchased from Sigma-Aldrich (St. Louis, MO), and Natural Pharmaceuticals (Beverley, MA), respectively. The Lipofectamine 2000 transfection kit (Invitrogen, Carlsbad, CA) was used according to the supplied protocol. Antibodies against human polo-like kinase 1 (Plk1), pro-caspase-3, pro-caspase-9, Ki67 and β-actin and goat anti-mouse IgG-HRP antibody were purchased from Santa Cruz Biotechnology, Inc., Santa Cruz, CA siRNAs targeting human Plk1 (si*Plk1*) (sense strand, 5′-UGAAGAAGAUCACCCUCCUUAdTdT-3′ and antisense strand, 5′-UAAGGAGGGUGAUCUUCUUCAdTdT-3′) and scrambled siRNA (si*Nonsense*) (sense strand, 5′-UUCUCCGAACGUGUCACGUdTdT-3′ and antisense strand, 5′-ACGUGACACGUUCGGAGAAdTdT-3′) were supplied by Shanghai GenePharma Co. Ltd. (Shanghai, China). Fluorescein-tagged siRNA (FAM-siRNA) was synthesized by modification of the 3′-end of the sense strand of the scrambled siRNA with fluorescein.

Particle size was characterized on a Malvern Zetasizer Nano ZS90 with a He−Ne laser (633 nm) and 90° collecting optics. Transmission electronic microscopy (TEM) was performed on a JEOL-2010 microscope with an accelerating voltage of 200 kV. The paclitaxel encapsulation efficiency was determined by the high performance liquid chromatography (HPLC) method after the drug-loaded micelles were lyophilized and dissolved in acetonitrile. The HPLC measurement was performed under the conditions as previously described.[36]

Polymer Synthesis. The triblock copolymer poly(ethylene glycol)-*b*-poly(ε-caprolactone)-*b*-poly(2-aminoethyl ethylene phosphate) was synthesized according to a previously described procedure.[26] The degree of polymerization of each block was determined to be 45, 80, and 10, respectively, according to the ^{1}H NMR spectrum using the reported method.[26] Thus, the polymer was designated as mPEG$_{45}$-*b*-PCL$_{80}$-*b*-PPEEA$_{10}$. ^{1}H NMR (DMSO-d_6, ppm): 1.29 (−C(O)CH$_2$CH$_2$C*H*$_2$CH$_2$CH$_2$O−), 1.53 (−C(O)CH$_2$-C*H*$_2$CH$_2$C*H*$_2$CH$_2$O−), 2.27 (−C(O)C*H*$_2$CH$_2$CH$_2$CH$_2$CH$_2$O−), 3.15 (−OCH$_2$C*H*$_2$NH$_3^+$Cl$^-$), 3.51 (−C*H*$_2$C*H*$_2$O−), 3.98 (−C(O)CH$_2$CH$_2$-CH$_2$CH$_2$C*H*$_2$O−), 4.30 (−OC*H*$_2$CH$_2$NH$_3^+$Cl$^-$, −P(O)OC*H*$_2$C*H*$_2$O−).

Preparation of Micellar Nanoparticles and Paclitaxel-Loaded Micellar Nanoparticles. Micellar nanoparticles and paclitaxel-loaded micellar nanoparticles were prepared by the solvent evaporation method. Briefly, triblock copolymer (10 mg) with or without paclitaxel was dissolved in 1 mL of tetrahydrofuran and stirred at room temperature for at least 2 h. Then, 10 mL of ultrapurified water (Millipore, 18.2 MΩ) was added dropwise into the stirring solution at a rate of 60 mL/h. The mixture was stirred for an additional 1 h, followed by removal of tetrahydrofuran. The solution was filtered through a 0.45 μm filter to remove free paclitaxel. The final volume was adjusted to 2 mL for further experiments.

Preparation of Micelleplex and Gel Retardation Assay. Micellar nanoparticles or paclitaxel-loaded micellar nanoparticles was diluted with Opti-MEM medium (Invitrogen) at different concentrations. Desired amount of siRNA (si*Plk1* or si*Nonsense*) in Opti-MEM medium was then mixed with equal volume of nanoparticles by gentle pipetting. The formed micelleplex was allowed to stand at room temperature for 20 min before use. The electrophoretic mobility of micelleplex was visualized on a UV illuminator with ethidium bromide staining after electrophoresis on a 2% (w/v) agarose gel for 20 min at 60 V in TAE buffer (40 mM Tris-HCl, 1% v/v acetic acid, 1 mM EDTA).

Cell Culture. The MDA-MB-435s tumor cell line from the American Type Culture Collection (ATCC) was used to evaluate the potency of the delivery system both *in vitro* and *in vivo*. Cells were cultured in Dulbecco's Modified Eagle Medium (DMEM, Gibco, Carlsbad, CA) with 10% fetal bovine serum (Gibco) at 37 °C with 5% CO_2.

Animals and Tumor Xenograft Model. Female BALB/c nude mice (4−6 weeks old) were purchased from Shanghai Experimental Animal Centre of Chinese Academy of Sciences (Shanghai, China), and all animals received care in compliance with the guidelines outlined in the *Guide for the Care and Use of Laboratory Animals*. The procedures were approved by the University of Science and Technology of China Animal Care and Use Committee.

To set up the tumor xenograft model, MDA-MB-435s cells were maintained in T-75 flasks (Corning Inc., NY) and passaged twice a week. Cells (5×10^6) were suspended in 100 μL of Dulbecco's PBS without calcium or magnesium and were administered by subcutaneous injection into the armpit of the mice. Tumor volume (mm^3) was determined by measuring length (l) and width (w) and calculated as $V = lw^2/2$. Tumor-bearing mice were used 12 days post-tumor inoculation in experiments, at which point tumor volumes reached around 50 mm^3.

***In vitro* Analysis of Codelivery of PTX and siRNA into Tumor Cells.** $^{Rho\text{-}paclitaxel}$micelleplex$_{FAM\text{-}siRNA}$ containing both Rhodamine-labeled paclitaxel and FAM-labeled siRNA was prepared as described

above. MDA-MB-435s cells (5×10^4 cells/well) were seeded in a 24-well tissue culture plate and incubated for 24 h at 37 °C in 5% CO_2, followed by adding the $^{Rho\text{-}paclitaxel}$micelleplex$_{FAM\text{-}siRNA}$ solution. At predetermined time intervals, cells were washed twice with PBS, lysed with trypsin-EDTA solution, and analyzed on a FACSCalibur flow cytometer (BD Biosciences, USA). The results were analyzed using WinMDI 2.9 software.

For confocal laser scanning microscopy (CLSM) observations, MDA-MB-435s cells (5×10^4 cells/well) were seeded in a 35 mm glass bottom culture dish (MatTek Corporation) and incubated for 24 h at 37 °C in 5% CO_2. $^{Rho\text{-}paclitaxel}$micelleplex$_{FAM\text{-}siRNA}$ was added and incubated with the cells for 2 h. After removal of the medium, cells were washed twice with the preheated PBS, then 4 mL of growth medium containing 1 μg/mL 4′, 6-diamidino-2-phenylindole (DAPI) was added. The cells were directly observed under a Zeiss LSM 710 confocal microscope (Carl Zeiss, Jena, Germany) using a 63× objective.

***In vitro* si*Plk1* Transfection and Analysis of Plk1 Expression.** MDA-MB-435s cells (5×10^4) were seeded in 24-well tissue culture plates and incubated at 37 °C in 5% CO_2 for 24 h to reach ~70% confluence. Various formulations were added and incubated with the cells for 24 h (for mRNA isolation) or 48 h (for protein extraction). The cellular levels of Plk1 mRNA and protein were assessed using quantitative real-time PCR (qRT-PCR) and Western blot, respectively.

In qRT-PCR analysis, total RNA from transfected cells was isolated using the RNeasy mini-kits (Qiagen, Germantown, MD) according to the protocol of manufacturer. Two micrograms of total RNA were transcribed into cDNA using the PrimeScript First Strand cDNA Synthesis Kit (Takara, Japen). Thereafter, 2 μL of cDNA was subjected to qRT-PCR analysis targeting Plk1 and glyceraldehyde 3-phosphate dehydrogenase (GAPDH) using the SYBR Premix Ex Taq (Perfect Real Time) (Takara). Analysis was performed using the Applied Biosystems StepOne Real-Time PCR Systems. Relative gene expression values were determined by the ΔΔCT method using StepOne Software v2.1 (Applied Biosystems). Data are presented as the fold difference in Plk1 expression normalized to the housekeeping gene GAPDH as the endogenous reference, and relative to the untreated control cells. Primers used in qRT-PCR for Plk1 and GAPDH are: Plk1-forward 5′-AGCCTGAGGCCCGATACTACCTAC-3′, Plk1-reverse 5′-ATTAGGAGTCCCACACAGGGTCTTC-3′, and GAPDH-forward 5′-TTCACCACCATGGAGAAGGC-3′, GAPDH-reverse 5′-GGCATGGACTGTGGTCATGA-3′. PCR parameters consisted of 30 s of *Taq* activation at 95 °C, followed by 40 cycles of PCR at 95 °C × 5 s, 60 °C × 30 s, and 1 cycle of 95 °C × 15 s, 60 °C × 60 s, and 95 °C × 15 s. Standard curves were generated and the relative amount of target gene mRNA was normalized to GAPDH mRNA. Specificity was verified by melt curve analysis.

In Western blot analysis, transfected cells were first washed twice with cold PBS, and then resuspended in 50 μL of lysis buffer (50 mM HEPES, pH 7.5, 150 mM NaCl, 1% Triton X-100, 10% glycerol, 1.5 mM $MgCl_2$, 1 mM EGTA) freshly supplemented with Roche's Complete Protease Inhibitor Cocktail Tablets. The cell lysates were incubated on ice for 30 min and vortexed every 5 min. The lysates were then clarified by centrifugation for 10 min at 12 000× *g*. The protein concentration was determined using the BCA Protein Assay Kit (Lot: 23250, Thermo, Madison, WI). Total protein (50 μg) was separated on 12% Bis-Tris-polyacrylamide gels and then transferred (at 300 mA for 45 min) to Immobilon-P membranes (Millipore, Bedford, MA). After incubation in 5% bovine serum albumin (BSA, Sigma-Aldrich) in phosphate buffered saline with Tween-20 (PBST, pH 7.2) for 1 h, the membranes were incubated in 1% BSA in PBS with monoclonal antibodies against Plk1 (1:500) overnight. After incubation in 1% BSA with goat antimouse IgG-HRP antibody (1:10 000) for 30 min, bands were visualized using the ECL system (Pierce).

Cell Proliferation and Apoptosis Analyses Post si*Plk1* Transfection. Cell proliferation after si*Plk1* transfection was determined by the tritiated thymidine (^{3}H-TdR) incorporation assay. MDA-MB-435s cells cultured in 24-well plates were treated for 72 h with paclitaxel dissolved in DMSO, ^{paclitaxel}micelleplex$_{siNonsense}$, ^{paclitaxel}micelleplex$_{siPlk1}$, the mixture of ^{paclitaxel}micelleplex$_{siNonsense}$ and micelleplex$_{siPlk1}$ with the paclitaxel dose ranging from 0.1 to 0.001 μg/mL. MDA-MB-435s cells treated with blank micelles and micelleplex$_{siNonsense}$ were used as controls. After the addition of ^{3}H-TdR (5 μCi/well) for 6 h, cells were harvested through a cell harvester (Shanghai Mosutech, Co. Ltd., China) and samples were measured for radioactivity using a Beckman LS 1701 liquid scintillation system (Beckman Coulter, Inc., Indianapolis, IN) and Bio-Safe II scintillation fluid (Research Products International Corp., Mount Prospect, IL). The results of the experimental and control groups were normalized to the untreated group.

For apoptosis analysis, MDA-MB-435s cells cultured in 24-well plates were treated with the above-mentioned formulations at a paclitaxel dose of 0.005 μg/mL. After 72 h of treatment, apoptotic cells were detected on flow cytometry using the Annexin V-FITC Apoptosis Detection Kit I (BD Biosciences, San Jose, CA), and the results were analyzed using WinMDI 2.9 software.

***In vivo* Fluorescence Imaging.** For *in vivo* imaging, female mice bearing MDA-MB-435s tumors were administered 400 μL of $^{Rho\text{-}paclitaxel}$micelleplex$_{FAM\text{-}siRNA}$, or equivalent free FAM-siRNA, or PBS by i.v. injection. Animals were placed onto the warmed stage inside of an IVIS light-tight chamber and anesthesia was maintained with 2.5% isoflurane. Image acquisition was performed at different time intervals on a Xenogen IVIS Lumina system (Caliper Life Sciences, USA). Results were analyzed using Living Image 3.1 software (Caliper Life Sciences).

Drug Distribution in Tumor Tissues and Tumoral Cells. The distributions of Rho-paclitaxel and FAM-siRNA in tumor tissues and tumoral cells were analyzed using FACS and CLSM. $^{Rho\text{-}paclitaxel}$micelleplex$_{FAM\text{-}siRNA}$ and other controls were intravenously injected into nude mice bearing MDA-MB-435s tumors. Twenty-four hours later, the mice were sacrificed and tumor tissues were collected. For CLSM analysis, the tissues were fixed in 4% paraformaldehyde overnight at 4 °C, and then immersed overnight in 30% sucrose solution. Tumor tissues were sectioned (6 μm thick) and counterstained with DAPI and imaged using a Zeiss LSM 710 confocal microscope using a 40× objective. For FACS analysis, tissues were placed into a cell culture dish containing 10 mL RPMI-1640 medium (without serum) and nontumor tissues were removed with sterile ophthalmological tweezers. The remaining tumor tissues were then transferred to a new dish and cut into small pieces. The fragments were resuspended in 20 mL RPMI-1640 medium (without serum). The pelleted materials were resuspended with 10 mL tumor cell digestion solution (1 mg/mL collagenase I) and incubated at 37 °C for 2 h with agitation. Tumor cells were thencollected by centrifugation at 1200 rpm for 6 min at room temperature and washed twice with PBS containing 1% FBS. Tumor cells were filtered through a 200-mesh sieve and analyzed on a FACSCalibur flow cytometer (BD Biosciences). The results were analyzed using WinMDI 2.9 software.

Tumor Suppression Study. Tumor-bearing mice were randomly divided into different groups, and treated with various formulations by i.v. injection every other day. The doses of si*Plk1* (or si*Nonsense*) and paclitaxel of each injection were fixed at 0.223 mg/kg and 0.667 μg/kg, respectively. Otherwise, the dose of si*Nonsense* was fixed at 0.223 mg/kg, but the doses of paclitaxel were gradually increased from 10× to 1000× of 0.667 μg/kg.

Detection of Pro-caspase-3, Pro-caspase-9 and Plk1 Expression in Tumor Tissues. Tumor tissues were collected 24 h after the last treatment, and lysed in 100 μL tissue lysis buffer (50 mM HEPES, pH 7.5, 150 mM NaCl, 1 mM EGTA, 2.5 mM EDTA, 10% glycerol, 0.1% Tween 20, 1 mM dithiothreitol, 10 mM glycerol 2-phosphate, 1 mM NaF and 0.1 mM Na_3VO_4) freshly supplemented with Roche's Complete Protease Inhibitor Cocktail Tablets. The lysates were incubated on ice for a total of 30 min and vortexed every 5 min. The lysates were centrifuged for 10 min at 12,000 *g* and the protein concentration was determined using the BCA Protein Assay Kit (Lot: 23250, Thermo). Total protein (50 μg) was then separated on 12% Bis-Tris-polyacrylamide gels and transferred to Immobilon-P membranes (Millipore, Bedford, MA) at 300 mA for 45 min. After incubation with 5% BSA in PBS for 1 h, the membrane was incubated in 1% BSA with monoclonal antibodies against either pro-caspase-9 (1:500) or pro-caspase-3 (1:500) overnight. The membrane was further incubated in 1% BSA with goat antimouse IgG-HRP antibody (1:10 000) for 30 min and visualized using the ECL system (Pierce).

To determine the Plk1 expression in tumor tissue after different treatments, tumor tissues were collected 24 h after the last injection. The tumor tissues were lysed and the total protein (50 μg) was separated and analyzed as described above except using a monoclonal antibody against Plk1 (1:500).

Statistical Analysis. All of the data represent mean values ± standard deviation of independent measurements. Statistical analysis was performed with a Student's *t*-test (two-tailed). Statistical significance was assigned at $p < 0.05$ (95% confidence level). The synergism of the combined therapy was evaluated by combination index (*c.i.*) method.[37,38] A *c.i.* of 1 indicates an additive effect between two agents, whereas a *c.i.* < 1 or *c.i.* > 1 indicates synergism or antagonism, respectively.

Acknowledgment. This work was supported by the National Basic Research Program of China (973 Program 2010CB934001, 2009CB930301, 2010CB912800), the National Natural Science Foundation of China (20974105, 50733003, 30921140312, 30830110), the Fundamental Research Funds for the Central Universities (WK2070000008) and the Ministry of Health, China (2009ZX09103-715). The authors thank Professor Xi-Qun Jiang at Nanjing University for assistance with confocal microscopy measurements.

Supporting Information Available: Additional experimental methods, Figures and Table. This material is available free of charge *via* the Internet at http://pubs.acs.org.

REFERENCES AND NOTES

1. Greco, F.; Vicent, M. J. Combination Therapy: Opportunities and Challenges for Polymer-Drug Conjugates as Anticancer Nanomedicines. *Adv. Drug Delivery Rev.* **2009,** *61*, 1203–1213.
2. Mauceri, H. J.; Hanna, N. N.; Beckett, M. A.; Gorski, D. H.; Staba, M. J.; Stellato, K. A.; Bigelow, K.; Heimann, R.; Gately, S.; Dhanabal, M.; *et al.* Combined Effects of Angiostatin and Ionizing Radiation in Antitumour Therapy. *Nature* **1998,** *394*, 287–291.
3. Lane, D. Designer Combination Therapy for Cancer. *Nat. Biotechnol.* **2006,** *24*, 163–164.
4. Rubinfeld, B.; Upadhyay, A.; Clark, S. L.; Fong, S. E.; Smith, V.; Koeppen, H.; Ross, S.; Polakis, P. Identification and Immunotherapeutic Targeting of Antigens Induced by Chemotherapy. *Nat. Biotechnol.* **2006,** *24*, 205–209.
5. Lebedeva, I. V.; Washington, I.; Sarkar, D.; Clark, J. A.; Fine, R. L.; Dent, P.; Curiel, D. T.; Turro, N. J.; Fisher, P. B. Strategy for Reversing Resistance to a Single Anticancer Agent in Human Prostate and Pancreatic Carcinomas. *Proc. Natl. Acad. Sci. U.S.A.* **2007,** *104*, 3484–3489.
6. Sengupta, S.; Eavarone, D.; Capila, I.; Zhao, G.; Watson, N.; Kiziltepe, T.; Sasisekharan, R. Temporal Targeting of Tumour Cells and Neovasculature with a Nanoscale Delivery System. *Nature* **2005,** *436*, 568–572.
7. Heidel, J. D.; Yu, Z.; Liu, J. Y.; Rele, S. M.; Liang, Y.; Zeidan, R. K.; Kornbrust, D. J.; Davis, M. E. Administration in Non-Human Primates of Escalating Intravenous Doses of Targeted Nanoparticles Containing Ribonucleotide Reductase Subunit M2 siRNA. *Proc. Natl. Acad. Sci. U.S.A.* **2007,** *104*, 5715–5721.
8. Rozema, D. B.; Lewis, D. L.; Wakefield, D. H.; Wong, S. C.; Klein, J. J.; Roesch, P. L.; Bertin, S. L.; Reppen, T. W.; Chu, Q.; Blokhin, A. V.; *et al.* Dynamic Polyconjugates for Targeted *in Vivo* Delivery of siRNA to Hepatocytes. *Proc. Natl. Acad. Sci. U.S.A.* **2007,** *104*, 12982–12987.
9. Davis, M. E.; Zuckerman, J. E.; Choi, C. H.; Seligson, D.; Tolcher, A.; Alabi, C. A.; Yen, Y.; Heidel, J. D.; Ribas, A. Evidence of RNAi in Humans from Systemically Administered siRNA *via* Targeted Nanoparticles. *Nature* **2010,** *464*, 1067–1070.
10. Love, K. T.; Mahon, K. P.; Levins, C. G.; Whitehead, K. A.; Querbes, W.; Dorkin, J. R.; Qin, J.; Cantley, W.; Qin, L. L.; Racie, T.; *et al*. Lipid-Like Materials for Low-Dose, *in Vivo* Gene Silencing. *Proc. Natl. Acad. Sci. U.S.A.* **2010,** *107*, 1864–1869.
11. Semple, S. C.; Akinc, A.; Chen, J. X.; Sandhu, A. P.; Mui, B. L.; Cho, C. K.; Sah, D. W. Y.; Stebbing, D.; Crosley, E. J.; Yaworski, E.; *et al*. Rational Design of Cationic Lipids for siRNA Delivery. *Nat. Biotechnol.* **2010,** *28*, 172–176.
12. Zimmermann, T. S.; Lee, A. C.; Akinc, A.; Bramlage, B.; Bumcrot, D.; Fedoruk, M. N.; Harborth, J.; Heyes, J. A.; Jeffs, L. B.; John, M.; *et al.* RNAi-Mediated Gene Silencing in Non-Human Primates. *Nature* **2006,** *441*, 111–114.
13. Li, S. D.; Chen, Y. C.; Hackett, M. J.; Huang, L. Tumor-Targeted Delivery of siRNA by Self-Assembled Nanoparticles. *Mol. Ther.* **2008,** *16*, 163–169.
14. Spankuch, B.; Heim, S.; Kurunci-Csacsko, E.; Lindenau, C.; Yuan, J.; Kaufmann, M.; Strebhardt, K. Down-Regulation of Polo-Like Kinase 1 Elevates Drug Sensitivity of Breast Cancer Cells *in Vitro* and *in Vivo*. *Cancer Res.* **2006,** *66*, 5836–5846.
15. Spankuch, B.; Kurunci-Csacsko, E.; Kaufmann, M.; Strebhardt, K. Rational Combinations of siRNAs Targeting Plk1 with Breast Cancer Drugs. *Oncogene* **2007,** *26*, 5793–5807.
16. Macdiarmid, J. A.; Amaro-Mugridge, N. B.; Madrid-Weiss, J.; Sedliarou, I.; Wetzel, S.; Kochar, K.; Brahmbhatt, V. N.; Phillips, L.; Pattison, S. T.; Petti, C.; Stillman, B.; *et al.* Sequential Treatment of Drug-Resistant Tumors with Targeted Minicells Containing siRNA or a Cytotoxic Drug. *Nat. Biotechnol.* **2009,** *27*, 643–651.
17. Saad, M.; Garbuzenko, O. B.; Minko, T. Co-Delivery of siRNA and an Anticancer Drug for Treatment of Multidrug-Resistant Cancer. *Nanomedicine (London, U.K.)* **2008,** *3*, 761–776.
18. Chen, A. M.; Zhang, M.; Wei, D. G.; Stueber, D.; Taratula, O.; Minko, T.; He, H. X. Co-Delivery of Doxorubicin and Bcl-2 siRNA by Mesoporous Silica Nanoparticles Enhances the Efficacy of Chemotherapy in Multidrug-Resistant Cancer Cells. *Small* **2009,** *5*, 2673–2677.
19. Meng, H. A.; Liong, M.; Xia, T. A.; Li, Z. X.; Ji, Z. X.; Zink, J. I.; Nel, A. E. Engineered Design of Mesoporous Silica Nanoparticles to Deliver Doxorubicin and P-Glycoprotein siRNA to Overcome Drug Resistance in a Cancer Cell Line. *ACS Nano* **2010,** *4*, 4539–4550.
20. Wang, Y.; Gao, S.; Ye, W. H.; Yoon, H. S.; Yang, Y. Y. Co-Delivery of Drugs and DNA from Cationic Core-Shell Nanoparticles Self-Assembled from a Biodegradable Copolymer. *Nat. Mater.* **2006,** *5*, 791–796.
21. Kaneshiro, T. L.; Lu, Z. R. Targeted Intracellular Codelivery of Chemotherapeutics and Nucleic Acid with a Well-Defined Dendrimer-Based Nanoglobular Carrier. *Biomaterials* **2009,** *30*, 5660–5666.
22. Zhu, C. H.; Jung, S.; Luo, S. B.; Meng, F. H.; Zhu, X. L.; Park, T. G.; Zhong, Z. Y. Co-Delivery of siRNA and Paclitaxel into Cancer Cells by Biodegradable Cationic Micelles Based on PDMAEMA-PCL-PDMAEMA Triblock Copolymers. *Biomaterials* **2010,** *31*, 2408–2416.
23. Chen, Y.; Wu, J. J.; Huang, L. Nanoparticles Targeted with NGR Motif Deliver C-Myc siRNA and Doxorubicin for Anticancer Therapy. *Mol. Ther.* **2010,** *18*, 828–834.
24. Chen, Y. C.; Bathula, S. R.; Li, J.; Huang, L. Multifunctional Nanoparticles Delivering Small Interfering RNA and Doxorubicin Overcome Drug Resistance in Cancer. *J. Biol. Chem.* **2010,** *285*, 22639–22650.
25. Patil, Y. B.; Swaminathan, S. K.; Sadhukha, T.; Ma, L. A.; Panyam, J. The Use of Nanoparticle-Mediated Targeted Gene Silencing and Drug Delivery to Overcome Tumor Drug Resistance. *Biomaterials* **2010,** *31*, 358–365.
26. Sun, T. M.; Du, J. Z.; Yan, L. F.; Mao, H. Q.; Wang, J. Self-Assembled Biodegradable Micellar Nanoparticles of Amphiphilic and Cationic Block Copolymer for siRNA Delivery. *Biomaterials* **2008,** *29*, 4348–4355.
27. Barr, F. A.; Sillje, H. H.; Nigg, E. A. Polo-Like Kinases and the Orchestration of Cell Division. *Nat. Rev. Mol. Cell Biol.* **2004,** *5*, 429–440.
28. Liu, X.; Erikson, R. L. Polo-Like Kinase (Plk)1 Depletion Induces Apoptosis in Cancer Cells. *Proc. Natl. Acad. Sci. U.S.A.* **2003,** *100*, 5789–5794.
29. Strebhardt, K.; Ullrich, A. Targeting Polo-Like Kinase 1 for Cancer Therapy. *Nat. Rev. Cancer* **2006,** *6*, 321–330.

30. Judge, A. D.; Robbins, M.; Tavakoli, I.; Levi, J.; Hu, L.; Fronda, A.; Ambegia, E.; McClintock, K.; MacLachlan, I. Confirming the RNAi-Mediated Mechanism of Action of siRNA-Based Cancer Therapeutics in Mice. *J. Clin. Invest.* **2009,** *119*, 661–673.
31. Matsumura, Y.; Maeda, H. A New Concept for Macromolecular Therapeutics in Cancer Chemotherapy: Mechanism of Tumoritropic Accumulation of Proteins and the Antitumor Agent Smancs. *Cancer Res.* **1986,** *46*, 6387–6392.
32. Dassie, J. P.; Liu, X. Y.; Thomas, G. S.; Whitaker, R. M.; Thiel, K. W.; Stockdale, K. R.; Meyerholz, D. K.; McCaffrey, A. P.; McNamara, J. O.; Giangrande, P. H. Systemic Administration of Optimized Aptamer-siRNA Chimeras Promotes Regression of PSMA-Expressing Tumors. *Nat. Biotechnol.* **2009,** *27*, 839–846.
33. Kim, S. H.; Jeong, J. H.; Lee, S. H.; Kim, S. W.; Park, T. G. Local and Systemic Delivery of VEGF siRNA Using Polyelectrolyte Complex Micelles for Effective Treatment of Cancer. *J. Controlled Release* **2008,** *129*, 107–116.
34. Poeck, H.; Besch, R.; Maihoefer, C.; Renn, M.; Tormo, D.; Morskaya, S. S.; Kirschnek, S.; Gaffal, E.; Landsberg, J.; Hellmuth, J.; *et al*. 5′-Triphosphate-siRNA: Turning Gene Silencing and Rig-I Activation against Melanoma. *Nat. Med.* **2008,** *14*, 1256–1263.
35. Jackson, A. L.; Linsley, P. S. Recognizing and Avoiding siRNA Off-Target Effects for Target Identification and Therapeutic Application. *Nat. Rev. Drug Discovery* **2010,** *9*, 57–67.
36. Wang, Y. C.; Tang, L. Y.; Sun, T. M.; Li, C. H.; Xiong, M. H.; Wang, J. Self-Assembled Micelles of Biodegradable Triblock Copolymers Based on Poly(Ethyl Ethylene Phosphate) and Poly(ε-Caprolactone) as Drug Carriers. *Biomacromolecules* **2008,** *9*, 388–395.
37. Chou, T. C.; Talalay, P. Quantitative Analysis of Dose-Effect Relationships: The Combined Effects of Multiple Drugs or Enzyme Inhibitors. *Adv. Enzyme Regul.* **1984,** *22*, 27–55.
38. Damaraju, V. L.; Bouffard, D. Y.; Wong, C. K.; Clarke, M. L.; Mackey, J. R.; Leblond, L.; Cass, C. E.; Grey, M.; Gourdeau, H. Synergistic Activity of Troxacitabine (Troxatyl) and Gemcitabine in Pancreatic Cancer. *BMC Cancer* **2007,** *7*, 121.